

## PROGRESS REPORT ON THE SLAC LINEAR COLLIDER\*

- W. Kozanecki

Stanford Linear Accelerator Center  
Stanford University, Stanford, California 94305

### 1. INTRODUCTION

In this paper we report on the status of the SLAC Linear Collider (SLC), the prototype of a new generation of colliding beam accelerators. This novel type of machine holds the potential of extending electron-positron colliding beam studies to center-of-mass (c.m.) energies far in excess of what is economically achievable with colliding beam storage rings. If the technical challenges posed by linear colliders are solvable at a reasonable cost, this new approach would provide an attractive alternative to electron-positron rings, where, because of rapidly rising synchrotron radiation losses, the cost and size of the ring increases with the square of the c.m. energy.

In addition to its role as a test vehicle for the linear collider principle, the SLC aims at providing an abundant source of  $Z^0$  decays to high energy physics experiments. Accordingly, two major detectors, the upgraded Mark II, now installed on the SLC beam line, and the state-of-the-art SLD, currently under construction, are preparing to probe the Standard Model at the  $Z^0$  pole.

The SLC project was originally funded in 1983. Since the completion of construction, we have been commissioning the machine to bring it up to a performance level adequate for starting the high energy physics program. In the remainder of this paper, we will discuss the status, problems and performance of the major subsystems of the SLC. We will conclude with a brief outline of the physics program, and of the planned enhancements to the capabilities of the machine.

### 2. PROJECT DESCRIPTION

The SLC [1] is not a linear collider in the truest sense, namely two linacs pointing at each other. Rather, it is an adaption of the existing SLAC facilities to which damping rings have been added near injection and transport lines have been added to the end of the accelerator to bring intense, very small phase space beams into collision.

A schematic view of SLC is shown in Fig. 1. The various subsystems are: an Electron Source to provide two high-intensity short pulses; a sector (1 of 30) of acceleration to bring the energy up to 1.2 GeV; two Damping Rings to reduce the phase space occupied by

---

\*Work supported by the Department of Energy, contract DE-AC03-76SF00515.

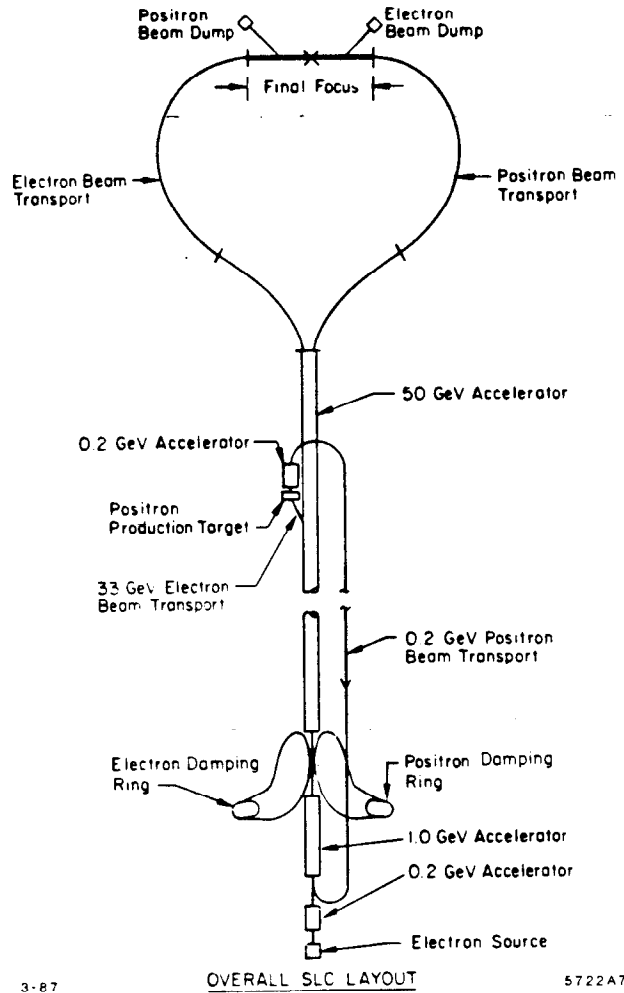


Fig. 1. Schematic Layout of the SLC.

the beams; the existing Linac modified to provide stronger focussing and beam guidance capability; higher power Klystrons for higher energy acceleration in the Linac; a new Positron Source system; an Arc transport line for each beam; and a Final Focus system to produce small beams and bring them into collision. In addition, there is a new control system with much improved capabilities needed to match the increased complexity of the machine.

Let us briefly trace the steps of an operating cycle beginning at a time when each of the two Damping Rings have circulating in them two damped bunches. Start the cycle by extracting one bunch of positrons from the south ring and, 59 ns later, extract both electron bunches from the north ring. Each Ring-to-Linac (RTL) transport line contains a longitudinal phase compressor which transforms the length of each bunch from its ring equilibrium value ( $\sigma_z = 6mm$ ) to about 1.5 mm, suitable for matching into the Linac RF structure.

The first two bunches ( $e^+, e^-$ ) are accelerated to the end of the Linac, transported around their respective Arcs, demagnified to transverse dimensions of a few microns in the Final Focus system and brought into collision at the Interaction Point (IP). Following their disruptive interaction the beams are extracted; their energy is precisely measured on each pulse; and they are finally discarded into a dump.

The third bunch, designated the scavenger bunch as it uses up some of the remaining RF in the Linac, is extracted two thirds of the way down the Linac and targeted to produce positrons. These positrons are collected and accelerated to 200 MeV in a high gradient, strongly focussed linear accelerator, then turned around and sent down a 2 km line to the beginning of the Linac for reinjection and subsequent acceleration to 1.2 GeV. Just prior to their arrival into the Linac, the electron gun is fired producing two bursts of particles spaced 62 ns apart which are bunched and also accelerated to 1.2 GeV for injection into their ring in which they are damped for 5 to 8 ms. The timing of these gymnastics is so arranged that the positrons enter their ring to replace the bunch that was extracted on the previous cycle. Having a larger transverse phase space to be damped, the positrons will remain in their ring twice as long as the electrons in theirs. At the start of the next cycle the alternate fully damped bunch is used.

Table I shows a brief summary of the critical design parameters, and of the progress to date, which we now proceed to evaluate in detail.

Table I. Basic Parameters of the SLC.

|                                      | Design Goal        | Initial Goal       | Achieved              | Units                            |
|--------------------------------------|--------------------|--------------------|-----------------------|----------------------------------|
| Beam Energy at IP                    | 50                 | 46                 | 46                    | GeV                              |
| Beam Energy at End of Linac          | 51                 | 47                 | 53                    | GeV                              |
| Electrons at Entrance of Arcs        | $7 \times 10^{10}$ | $1 \times 10^{10}$ | $3.5 \times 10^{10}$  |                                  |
| Positrons at Entrance of Arcs        | $7 \times 10^{10}$ | $1 \times 10^{10}$ | $0.6 \times 10^{10}$  |                                  |
| Repetition Rate                      | 180                | 60                 | 5                     | Hz                               |
| Bunch Length<br>$\sigma_s$           | 1.5                | 1.5                | 1.5 - 3.0             | mm                               |
| Transverse Emittance at End of Linac | $3 \times 10^{-5}$ | $5 \times 10^{-5}$ | $3-20 \times 10^{-5}$ | mrad                             |
| Spot Radius at IP                    | 1.6                | 2.8                | ~6                    | Microns                          |
| Luminosity                           | $6 \times 10^{30}$ | $6 \times 10^{27}$ | —                     | $\text{cm}^{-2} \text{sec}^{-1}$ |
| Z <sup>0</sup> 's per day            | $1.5 \times 10^4$  | 15                 | —                     |                                  |

### 3. STATUS OF COMMISSIONING OF THE MAJOR SLC SYSTEMS

Specialized descriptions of the various SLC subsystems, as well as in-depth analyses of the performance to date, have been reported recently [2-5]. We have therefore opted, in this section, for a more qualitative discussion of the machine physics issues. No attempt has been made to refer to all contributing individuals, nor to quote all published or unpublished documents. Many of the results summarized below are reported in more detail in numerous reports at other conferences [6].

#### 3.1 INJECTION

The SLC injector [7] consists of the electron source and the first of the 30 Linac sectors. The source must produce a pair of intense electron bunches ( $\geq 7 \times 10^{10} e^-$  per pulse), with time separation (62 ns), emittance ( $1.8 \times 10^{-3}$  m-rad), and momentum spread ( $\pm 1\%$ ) appropriate, after acceleration to 1.2 GeV, for injection into the North Damping Ring. Positrons, which have been injected at 200 MeV into the Linac, must be accelerated along with the electron bunches and transported into the South Damping Ring. Control of the energies and energy spread of the three bunches are required for efficient injection into the rings. Intensity stabilization is important in the control of the energy jitter of the beams extracted from the damping rings. In addition, proper adjustment and stabilization of the temporal spacing of the bunches is necessary so that colliding beams always cross at the same location in the interaction hall.

As of June 1987, properly spaced pairs of electron bunches can be accelerated and stabilized in energy for injection into the North Damping Ring. Emittance and momentum spread requirements (for 120 Hz operation) are met without difficulty for bunch populations of  $5 \times 10^{10} e^-$ . At bunch populations in excess of  $7.5 \times 10^{10}$ , intensity jitter becomes a problem.

Positron transmission through the injector region depends upon the initial positron launch conditions. An increased positron bunch length enlarges the energy spread which results in poor transmission and injection into the south ring. Transmission efficiencies through the injector into the ring of 40% are typically achieved. This is expected to improve as the positron source is brought up to full specifications.

Whereas double electron bunch operation has been tested, only single bunches are routinely accelerated through the injector region. Two-bunch operation is awaiting the installation of a two bunch extraction kicker in the North Damping Ring. Testing of three bunch operation is scheduled for the Fall of 1987. Tests of the polarized  $e^-$  source are planned for 1988.

#### 3.2. DAMPING RINGS

Two damping rings [8] have been built to reduce the transverse emittance of the positron and electron bunches to a value of  $\gamma\epsilon = 3 \times 10^{-5}$  m-rad required for micron sized spots at the IP. At 120 Hz, 8.3 msec are available for damping. In the electron ring, two bunches must be damped simultaneously, as well as injected into and extracted from orbits separated by half the circumference of the ring. In addition, the length of bunches of electrons and positrons must be shortened to 1.5 mm between extraction from the ring and reinjection into the Linac.

Initial commissioning of both rings is complete. Transverse emittance requirements for operation at 120 Hz are readily achieved during available damping time, as shown in Fig. 2. The electron ring routinely delivers single bunches of  $2 - 3 \times 10^{10}$  electrons for recirculation in the Linac. The positron ring and transfer lines typically output  $4 \times 10^9$  positrons; their transmission (typically 50%) remains to be optimized.

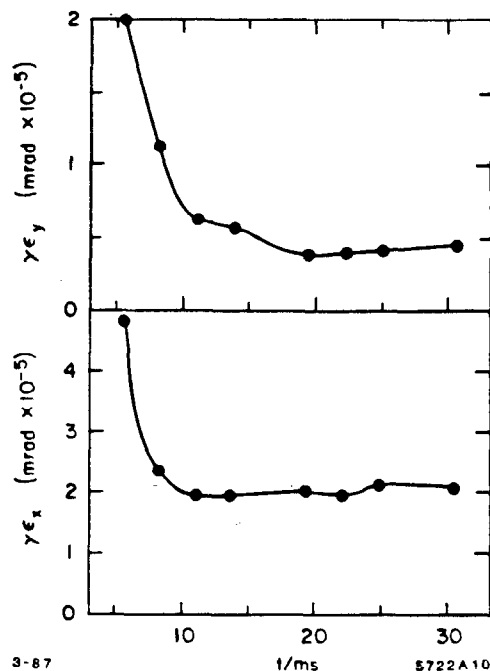


Fig. 2. The emittance of the beam extracted from the electron storage ring as a function of storage time. Design emittance is  $3 \times 10^{-5}$  m-rad. The vertical emittance  $\gamma\epsilon_y$  is smaller than the horizontal emittance because the Ring is operated without coupling.

Bunch lengthening, which reduces the maximum usable current to about  $2 \times 10^{10}$  particles per pulse, has been observed (Fig. 3) in both Damping Rings. This dependence of the bunch length on current is caused by an excessive longitudinal ring impedance, due to too narrow a vacuum pipe through the bending magnets, and to too many transitions between vacuum chambers of varying sizes. Even though it is possible to extract higher currents from the ring, it is not possible to compress the large bunch lengths in the transport line leading from the rings to the Linac (RTL) because of energy aperture restrictions in the RTL. Furthermore, the minimum achievable bunch length is limited by the equilibrium energy spread which increases above the turbulence threshold (about  $1.5 \times 10^{10}$  e/bunch).

An increased longitudinal beam size results in larger momentum spread in the Linac, and in increased sensitivity to transverse wake fields. In addition, the increased scavenger bunch length results in increased positron bunch lengths which are subsequently difficult to inject into the south damping ring because of an enlarged energy spread. The present system is adequate for operation at  $1 \times 10^{10}$  particles per pulse. The maximum useful beam current can be increased to nearly  $5 \times 10^{10}$  by shielding the ring bellows; enlarging the RTL energy aperture (this is currently being implemented); increasing the available RF

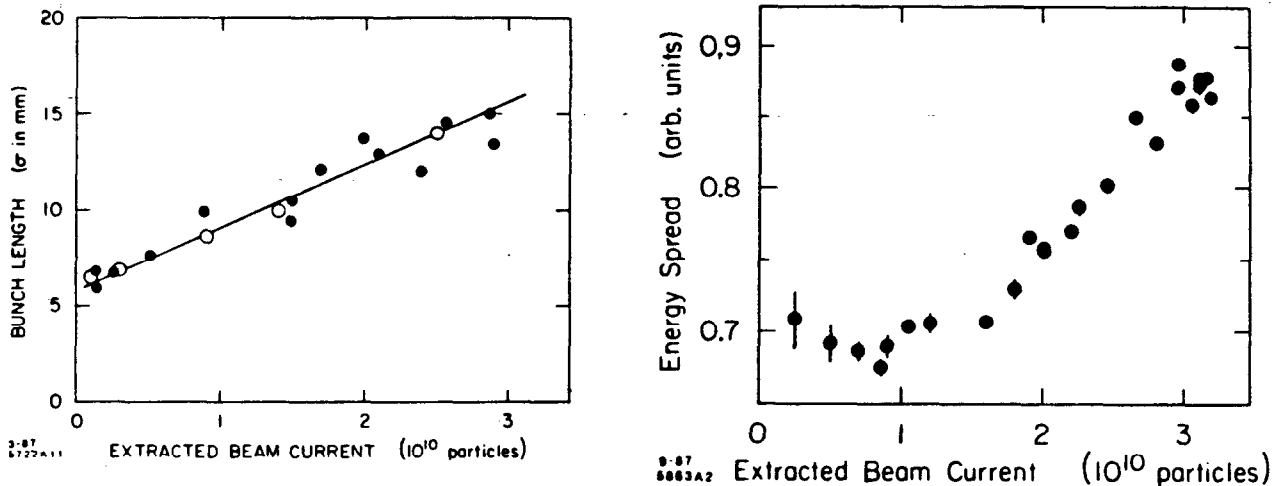


Fig. 3. (a) Equilibrium bunch length in the Damping Rings as a function of beam current. Design bunch length is 6 mm at this location. (b) Equilibrium energy spread in the Damping Rings as a function of beam current. A threshold for turbulent bunch lengthening is observed at about  $1.5 \times 10^{10}$  particles/bunch.

voltage in the ring; and performing some precompression in the ring itself by inducing a properly timed quadrupole oscillation (this has been successfully demonstrated). Reaching the ultimate design goal of  $7 \times 10^{10}$  particles per pulse will require a substantial redesign of the damping ring vacuum chamber to minimize the longitudinal ring impedance.

The SLC specifically calls for the simultaneous injection and extraction of two electron bunches separated by half a ring circumference. Two-bunch injection and storage has been successfully demonstrated. During the present Autumn 1987 shutdown a new extraction kicker will be installed which will permit simultaneous extraction of the two bunches and, hence, operation at 120 Hz. Without successful injection and extraction of two electron bunches, operation would be limited to 60 Hz, where alternate Linac cycles at 120 Hz accelerate alternate bunches of electrons for production of positrons and for transport to the interaction point.

### 3.3. POSITRON SOURCE

The SLC positron source [1,9] consists of a W-Re target, a flux concentrator, 200 MeV of acceleration and a 2 km return line. At the two-thirds point in the Linac, 33 GeV electrons are deflected onto the target. Positrons in the resultant shower are accelerated to 200 MeV in a s-band, high gradient capture section followed by three standard SLAC sections. The positrons are then transported back to the beginning of the Linac for subsequent acceleration to 1.2 GeV and injection into the South Damping Ring.

To date, a yield of one positron injected into the Linac from the South Damping Ring for every two electrons incident on target has been achieved. The maximum number of positrons stored in the south ring has been approximately  $1 \times 10^{10}$  particles in a single pulse. In order to accomplish this yield, careful tuning of the positron bunch length was required [3]. The smallest achieved bunch lengths are approximately 1.5 times longer than can be expected to fit inside the damping ring energy aperture after acceleration through the injector.

Reduction of the incident electron bunch length, installation (currently in progress) of a new high gradient section and capture region solenoid, as well as improved positron orbit control through the injector region are expected to bring the yield of damped positrons up to nearly one positron per electron incident on target.

### 3.4. LINAC

The SLAC Linac has been upgraded [2,10-12] to accelerate tightly focussed beams of positrons and electrons on the same RF pulse without significant emittance increase. Over 200 new 67 MW klystrons have been installed in the Linac, and beam energies of 53 GeV have been measured [13];  $3.5 \times 10^{10}$  electrons and  $0.4 \times 10^{10}$  positrons per bunch can be routinely accelerated to 47 GeV.

The transverse shapes of the beams at the end of the Linac depend on input conditions from the RTL, the quadrupole lattice, the energy-acceleration profile of the Linac and transverse wake fields. The transverse beam emittances have been measured at the end of the Linac as a function of beam current. At low intensity, the apparent electron emittance lies between one half (in the vertical plane) and four times (in the horizontal plane) the design value. This increase in apparent horizontal emittance between the exit from the damping ring and the exit from the Linac is attributed to residual unmatched dispersion in the RTL, which can be eliminated by careful tuning.

Above about  $0.8 \times 10^{10}$  electrons per pulse the bunch lengthening (due to the damping ring) increases the beam energy spread dramatically in the Linac, resulting in sharply increased chromatic phase dilution effects. Transverse wake field instabilities are also intensified by longer bunches. Previously mentioned improvements to the Damping Rings should reduce these problems and improve the apparent emittance above  $10^{10}$  particles per bunch.

Transverse wake fields, which arise from space charge effects in the accelerating structure, can displace the phase space of the trailing part of a bunch relative to the phase space of the leading part, effectively causing the bunch to grow a transverse tail [3,14]. The size of the effect depends on bunch current, bunch length and the accuracy with which the beam is launched into, and centered in, the accelerating structure. This effect has been studied experimentally in some detail; measurements agree quantitatively with expectations [3].

In order to keep transverse wake fields from diluting the phase space, strong focussing and accurate beam centering within the Linac irises is necessary. The Linac has, therefore, been instrumented with a new orbit control system designed to center the beam with an RMS error less than 100 microns. Performance to date is 125 microns for single beams (dominated by electronic calibration uncertainties) and about three times as much for two-beam operation (dominated by mechanical misalignments and by steering algorithm performance). Orbit quality is steadily improving.

In addition to "static" orbit control, "dynamic" corrections are necessary to compensate slow (e.g., temperature drifts) and fast changes (e.g., due to ripple on power supplies or changing klystron populations) in machine conditions. For instance, the launch of both positrons and electrons into the Linac from the Damping Rings and into the Arcs from the Linac must be controlled with feedback systems. Presently the position and angle of electrons into and out of the Linac are controlled once per minute by so-called slow feedback processes. An energy feedback system maintains the beam energy within 0.1% of nominal. The energy spread of the bunch currently meets the design value ( $\pm 0.2\%$ ) for bunch intensities less than about  $1 \times 10^{10}$ ; at higher intensities, the energy spread is limited by the increase in bunch length with bunch current. A fast feedback on the energy of the

electrons operating on a pulse-by-pulse basis has been shown to limit the RMS energy jitter to less than 0.13% [15], and is now being incorporated in the online control system.

The slow feedback processes for positrons are now just starting to be commissioned. Fast pulse-by-pulse feedback on the positron energy and the wake field-induced beam tails are also being installed.

The techniques for transverse stabilization described in this section are expected to prove effective for up to a few times  $10^{10}$  particles per bunch. Wake field control at the full design current will require the application of more sophisticated techniques, such as Landau damping; these lie beyond the scope of this report.

### 3.5. ARCS

The SLC Arc System [16-18] is designed to transport beams of electrons and positrons from the end of the SLAC Linac to the beginning of the Final Focus System where they are made to collide head on. To minimize phase space dilution caused by quantum fluctuations in the synchrotron radiation energy loss mechanism, the bending radii are large, and very high gradient AG cells are arranged in trains of low dispersion, terrain following, achromats.

Each Arc consists of about 240 identical cells; each cell, in turn, contains two very high gradient, combined function magnets, alternately focussing and defocussing. The relative strengths of the dipole, quadrupole and sextupole components of these magnets are set by the joint requirements of enforcing the designed beam trajectory, maintaining the proper betatron phase advance in both vertical and horizontal planes, and achieving the delicate balance of high order cancellations that ensure achromatic behavior. As the dipole and quadrupole fields experienced by the beam depend on the orbit itself, the above requirements imply tight tolerances on the alignment of the magnets. This, and the necessity to avoid separate steering correctors that take up additional space, lead to a design that incorporates mechanical magnet movers: these remotely adjust the vertical (or horizontal) position of each magnet to simultaneously optimize the beam trajectory and the betatron phase advances.

Early stages of Arc commissioning suffered from poor reproducibility of magnet mover settings, and from very slow mechanical deformations of a few percent of the magnets, that caused gross misalignments. The worst of these mechanical failures have now been mended. At the present stage, random alignment errors in the electron Arc, based on detailed orbit and optical measurements, are estimated not to exceed 150 microns RMS (the design calls for a tolerance of 100 microns). Systematic errors in the placement of the magnetic centers, originally found at the 200 to 400 micron level, have mostly been removed by experimentally tuning the betatron phase advance along the Arc. With the exception of a few badly behaved cells, which remain to be corrected, the present alignment of the electron Arc is adequate for achieving a 2 to 4 micron spot size at the IP.

Optical performance of the Arcs is very sensitive to phase shift errors through the lattice. This problem arises because the beam line does not lie in a plane; instead, it follows the local terrain. At each roll, i.e., at each point where the radius of curvature of the Arc changes planes, cross-plane coupling occurs between the horizontal and vertical betatron oscillations. This coupling is in principle reversed at a downstream compensating roll, where the radius of curvature returns to the original plane; however, this cancellation occurs only if the total phase advance between rolls, lies in (each plane) within a few degrees of its design value of  $N * 2\pi$ . Otherwise, the strength of the coupling and the amplitude of the betatron oscillation increase to a point where the betatron phase space is



so distorted it can no longer be corrected by the Final Focus optics. This is illustrated in Fig. 4, where a deliberately induced horizontal betatron oscillation at the beginning of the Arc couples into the vertical plane by a roll. In Fig. 4a the coupling is eliminated after the compensating roll because the phase shift error is small. In Fig. 4b, a phase shift error causes residual coupling. By adjusting magnet positions and correction coil excitations, phase shift errors have been corrected in the electron Arc. A similar procedure will be applied to the positron Arc.

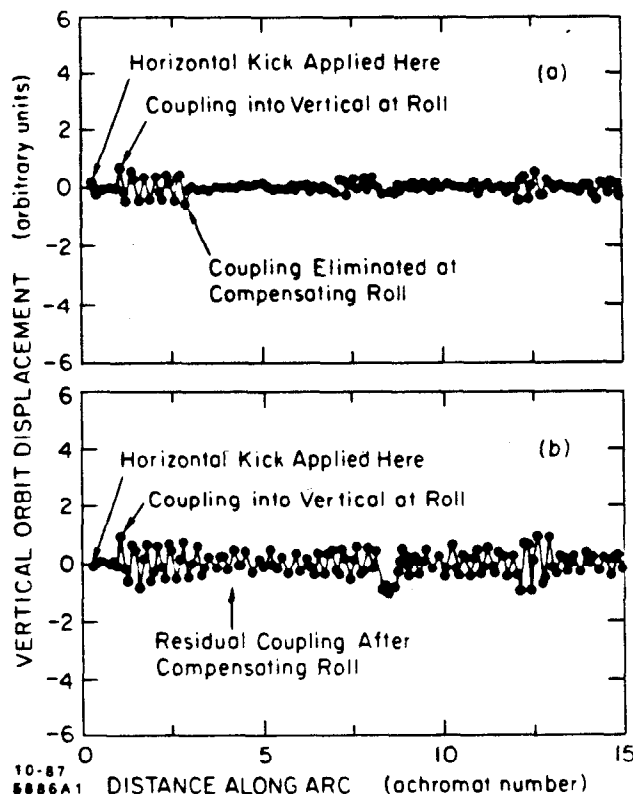


Fig. 4. Vertical beam orbit displacement as a function of distance along the Arc for a beam to which a horizontal kick has been applied at the entrance to the Arc. The horizontal oscillation couples into the vertical at a magnet roll. If the phase shift error is small, as in (a), the coupling is eliminated at the compensating roll. If a residual phase shift error exists, as in (b), the coupling remains beyond the compensating roll.

Studies are in progress on several fronts to reduce the sensitivity of the Arcs to gradient errors and to misalignments. For instance, adiabatic transitions at roll boundaries, spread over several magnets, have been demonstrated to provide local compensation of couplings; direct position readout of each magnet in both planes, as well as increased sampling frequency of the beam trajectories in each plane, greatly improve the diagnostic of so far undetected systematic errors. Such upgrades are to be progressively implemented over the next twelve months, and are expected to bring the system, from its present state that is adequate for low luminosity running, up to full SLC specifications.

### 3.6. FINAL FOCUS

The Final Focus system, filling the last 150m of tunnel on either side of the IP, contains the elements that demagnify the beams to a final spot size of about 2 microns, steer them into collision, and transport the disrupted outgoing beams to the dumps.

The optical design [19] utilizes telescopic modules with simultaneous point to point and parallel to parallel focussing, to minimize the magnitude of high order optical distortions [20]. More specifically, each arm consists of a dispersion-matching section, followed by a first level of demagnification which also completes, in betatron space, the matching of the incoming Arc beam. At this stage, most optical imperfections due to machine irregularities upstream have been corrected [21]. The beam then traverses a chromatic correction section, whose purpose is to precisely balance the chromatic aberrations introduced by the high demagnification, short focal length final telescope. For nominal incoming emittance, the expected beam size at the IP is  $\sigma = 2.4$  microns with the current optics, and should reach 1.8 microns when the superconducting final telescope is installed in 1989.

Commissioning to date has concentrated on single beam optical issues. Dispersion matching routinely yields a dispersion function within a few percent of the design; betatron matching, on the other hand, has been only moderately successful, as the quality of the electron beam delivered by the North Arc does not yet routinely bring it within correction range. In spite of these difficulties, spot sizes of four to six microns have been measured (Fig. 5) at the collision point, by scanning a thin carbon fiber of 3.5 micron radius across the beam, and recording the beam-induced secondary emission signal. These beam sizes, equal to two to three times the design beam size, are the smallest that can be theoretically achieved, with design emittances, and with the chromatic correctors left off, as was indeed the case. This surprisingly simple measurement establishes that the basic optics, throughout the machine, is essentially sound.

While most studies in the Final Focus have so far concentrated on electrons, a positron spot of 20 microns, in both dimensions, has been recorded at the IP. In addition,

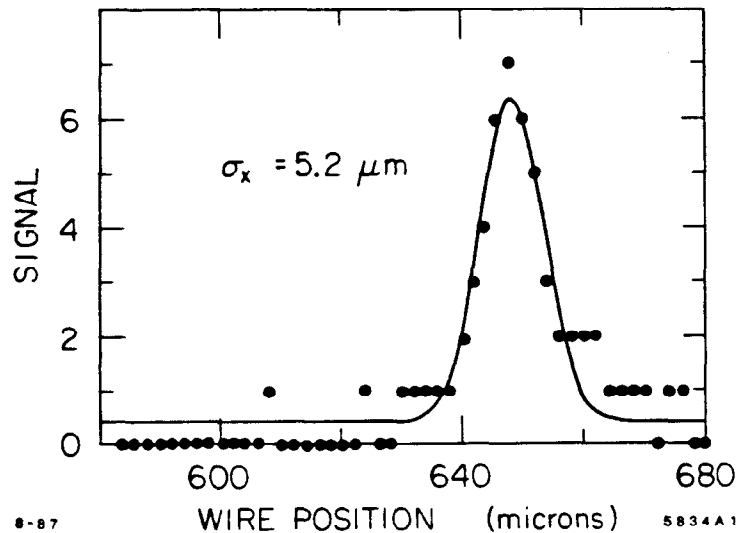


Fig. 5. A transverse scan of the beam at the SLC collision point with the 3.5 micron radius wire. Unfolding the wire size contribution gives an RMS beam size of 4.6 microns.

both beams were maintained in "collision," for several hours, within a few ten microns of each other in the transverse plane. This allowed the longitudinal position of the collision point to be measured, by timing techniques, to lie well within tolerance (less than 2 mm) of its design location.

One of the most severe challenges of linear colliders is to measure, and bring into collision, beams of the minute sizes needed to produce luminosity. While in storage rings, constraints inherent to the machine itself almost force the beams into collision, no such recourse is available here; in addition, as the center-of-mass energy increases, the once prolific Bhabha scattering cross section no longer provides a sensitive enough luminosity monitor.

As previously mentioned, single beam profiles have been measured with thin carbon fibers scanning across the beam. Such a device, consisting of two wire-carrying heads at right angles to each other, is being installed inside the Mark II detector. Each head carries three wires (12.5, 3.5 and 2 microns radius, respectively), and can be remotely "flipped" into the beam path; the beam is then scanned magnetically across one of the wires. The heads are disposed such that one of them measures horizontal profiles, while the other head measures the vertical beam size. Great care has been exercised in order to minimize the amount of material within the solid angle acceptance of the central Mark II drift chamber.

Let us now turn to beam-beam finding. Once both beam profiles have been optimized using the wire scanner, the beams are brought within about 10 microns of each other, guided by two strip-line beam position monitors (BPM) located about a foot on either side of the IP. Further optimization of beam-beam centering is then achieved by taking advantage of the beam-beam deflection [21]: unless the two beams are colliding exactly head-on, they deflect each other by angles of the order of 0.2 mrad. This deflection, amplified by a 5 m lever arm, is detected in BPM's captured inside the final telescope, that simultaneously measure both beams on each pulse, and detect the displacement of, say, the electron beam, as the positron beam is scanned across it. The magnitude of the effect depends, as illustrated in Fig. 6, on the beam current, on the distance between the two beams, and on the spot size (diffuse clouds will deflect each other less than line charges would). It therefore constitutes a very powerful diagnostic for optimizing the luminosity.

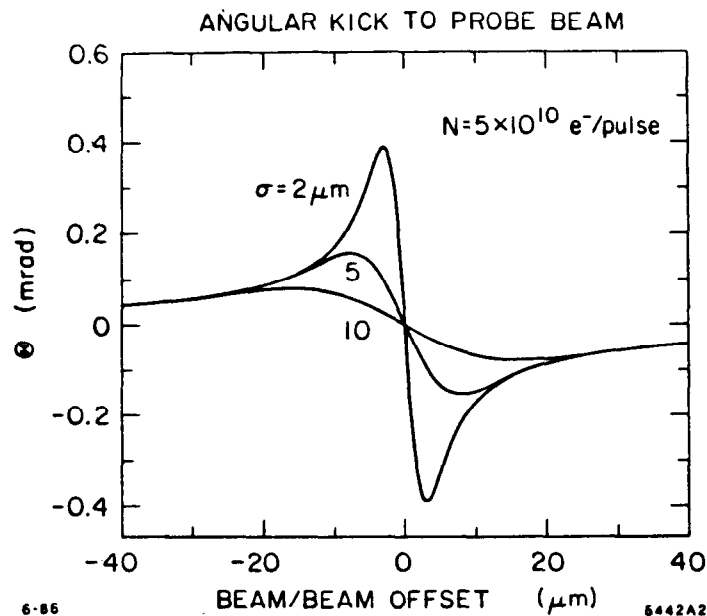


Fig. 6. Beam-beam deflection angle vs. offset for three different spot sizes.

Another diagnostic of the beam-beam interaction is also available. At equivalent luminosities of about  $5 \times 10^{27}$ , the electromagnetic field induced by one beam onto the other is sufficient to induce detectable synchrotron radiation, termed "beamstrahlung". At the SLC, we have installed threshold Cherenkov counters beyond the first bending magnet on either side of the IP. These monitors will measure the total beamstrahlung photon flux above 20 MeV (which strongly depends on the beam size), and the mean photon direction (which can be used for beam-beam steering). The 20 MeV threshold is chosen to eliminate the very intense, but much lower energy, synchrotron radiation from the bending magnets.

#### 4. EXPERIMENTAL PHYSICS PROGRAM AND FUTURE PLANS

$Z^0$  physics at the SLC will begin with an upgraded PEP detector, the Mark-II, to be followed by a new, state-of-the-art experiment, the SLD.

The Mark II detector [4,22] consists of the following components (Fig. 7). A new central drift chamber [23] provides greatly improved tracking accuracy, extended angular coverage, two-particle separation, and  $\pi - e$  identification by  $dE/dx$ . A new magnet coil restores the central solenoidal field to 5 kGauss. Electromagnetic calorimetry, which previously covered only the central region, has been extended to forward angles by the addition of an endcap electromagnetic calorimeter, of small angle monitors and of instrumented radiation masks. The muon system coverage has improved by about 40 %. The time of flight system has been outfitted with new scintillators. Finally, a high pressure drift chamber and a silicon strip vertex detector, to be installed next summer, will take advantage of the very small transverse size of the collision region for heavy flavor studies. With the exception of the vertex detectors and of the small angle monitors, the fully upgraded MarkII has undergone extensive tests both with cosmic rays and with electron-positron beams at PEP, where it collected  $30 \text{ pb}^{-1}$  of physics-quality data. At the time of this writing, the detector is installed on the SLC beam line, ready to record physics data. Because of the PEP test run, we expect the time between the first production of  $Z^0$ 's, and the production of good quality data for analysis, to be considerably shorter than would be required for a new and untested facility.

A new and potentially much more capable detector, the SLD [24], is under construction. Compared to the Mark II, its main advantages are: full solid angle electromagnetic and hadronic calorimetry; particle identification up to very high momenta through the use of Cherenkov Ring Imaging; and a very high resolution, two-dimensional, CCD-based vertex detector. The SLD, which also requires the installation of a superconducting final telescope at the Final Focus, is expected to move onto beam line in approximately two years.

Expressed in terms of parameters at the interaction point, the luminosity is:

$$\mathcal{L} = \frac{N^+ N^-}{4\pi\sigma^2} f H$$

where  $N^+$  and  $N^-$  are the number of particles in the colliding bunches of positrons and electrons,  $\sigma$  is the RMS beam radius,  $f$  is the frequency of collision, or repetition rate, and  $H$  is the enhancement factor which represents the increase in luminosity due to the focussing of the beams in the fields of each other. The physics program is expected to begin in earnest when the machine reaches about  $10^{-3}$  of its design luminosity, corresponding to 15 produced  $Z^0$  per day. The luminosity will then progressively improve as machine development and data taking alternate. The integrated exposure for Mark II is projected to reach about  $10^5 Z^0$ 's, appropriate for exploratory physics. SLD plans to collect an order

of magnitude more data, by drawing on higher beam currents, stronger focussing at the IP, the onset of luminosity pinch enhancement, and longer running time.

Two improvements to the physics capabilities of SLC are under construction. Firstly, an energy spectrometer [25] is being installed in each of the Final Focus extraction lines. It will measure the energy of each beam on a pulse-to-pulse basis. The estimated absolute accuracy of the c.m. energy measurement (and, hence, of the  $Z^0$  mass) is 45 MeV, dominated by systematics of magnet alignment and of residual dispersion at the IP.

The second improvement project is the development of a longitudinally polarized electron beam [26]. A polarization of the electrons of  $P = 45\%$ , controlled to  $\delta P/P = \pm 1\%$ , of the electrons, is equivalent, for asymmetry studies, to about a factor of 100 gain in integrated luminosity. The SLC Polarization Group aims to have all components of this facility fabricated, installed and tested by the end of 1988.

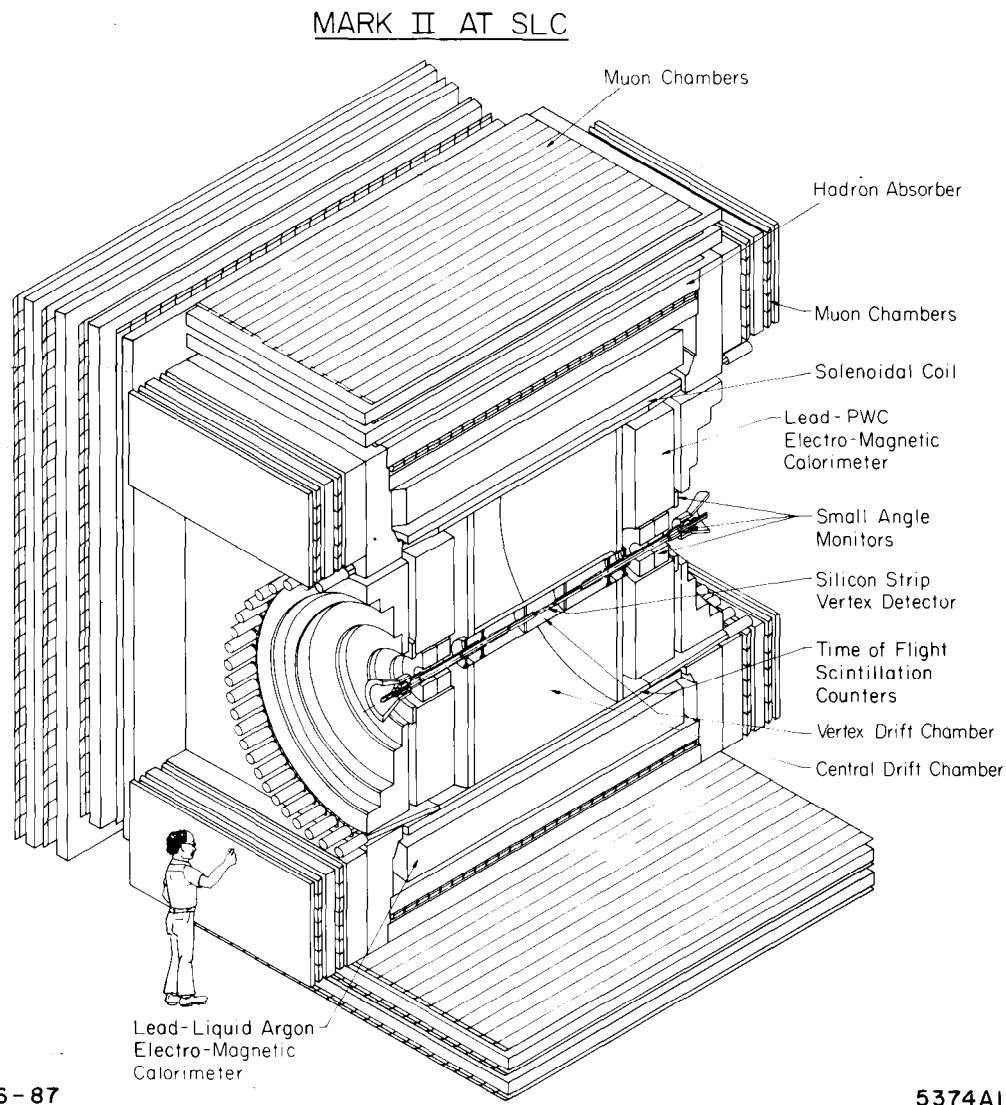


Fig. 7. Cut-away view of the Mark II detector.

## ACKNOWLEDGEMENTS

In preparing this talk, I have drawn on the work of many of my SLC colleagues. I would like to thank in particular S.Ecklund, G.Fischer, A. Hutton, J. M. Paterson, J. Seeman, J. C. Sheppard and R. Stiening, with whom I share the daily fun and excitement of this enterprise. The organizers of this Conference have provided for an inspiring, lively, and, last but not least, sunny working atmosphere in beautiful Uppsala. Jag skulle vilja tacka dem for detta !

## REFERENCES

1. SLC Design Handbook, Stanford Linear Accelerator Center, Stanford, December 1984.
2. R. Stiening, SLAC-PUB-4263, March 1987, to be published in Proceedings of the 12th Particle Accelerator Conf., Washington, D. C., March 16-19, 1987.
3. J. T. Seeman and J. C. Sheppard, Proceedings of the Workshop on New Developments in Particle Accelerator Techniques, Orsay, France, June 29-July 4, 1987.
4. A. Lankford, Status of the SLAC Linear Collider and of the Mark II Detector, 7th International Conf. on Physics in Collision, Tsukuba, Japan, Aug. 25-27, 1987, SLAC-PUB-4450, Oct.1987.
5. B. Richter and R. Stiening, The SLAC Linear Collider — A Status Report, invited talk presented by B. Richter at the 1987 International Symposium on Lepton and Photon Interactions at High Energies, Hamburg, Germany, July 27-31, 1987, SLAC-PUB-4367, July 1987.
6. Proceedings of the 1985 Particle Accelerator Conference, Vancouver, B. C., Canada, May 13-16, 1985; Proceedings of the Stanford Linear Accelerator Conference, Stanford, June 1986; Proceedings of the 12th Particle Accelerator Conference, Washington, D. C., March 16-19, 1987.
7. J. C. Sheppard *et al.*, Commissioning the SLC Injector, Proc. of the 12th Particle Accel. Conf., Washington, D. C., March 16-19, 1987.
8. G. E. Fischer *et al.*, A 1.2-GeV Damping Ring Complex for the Stanford Linear Collider, Proc. 12th Int. Conf. on High Energy Accel., FNAL, 37 (1983).
9. F. Bulos *et al.*, Design of a High Yield Positron Source, IEEE Trans. Nucl. Sci., NS-32, 1832 (1985).
10. J. T. Seeman *et al.*, Experimental Beam Dynamics in the SLC Linac, Proc. Particle Accel. Conf. (Washington, D. C., March 1987).
11. G. E. Fischer, SLC: Status and Development, Proceedings of the International Conference on High Energy Accelerators, Novosibirsk, U.S.S.R., August 1986.
12. J. T. Seeman and J. C. Sheppard, Special SLC Linac Developments, Proc. of the — Stanford Linear Accelerator Conference, Stanford, June 1986.
13. M. Allen *et al.*, Performance of the Stanford Linear Collider Klystrons at SLAC, Proc. Particle Accel. Conf. (Washington, D. C., March 1987).
14. J. T. Seeman *et al.*, Transverse Wakefield Control and Feedback in the SLC Linac, Proc. Particle Accel. Conf. (Washington, D. C., March 1987).

15. G. Abrams *et al.* Fast Energy and Energy Spectrum Feedback in the SLC Linac, Proc. Particle Accel. Conf. (Washington, D. C., March 1987).
16. G. E. Fischer *et al.*, Some Experiences from the Commissioning Program of the SLC Arcs, Proc. of the 12th Particle Accelerator Conf., Washington, D. C., March 16-19, 1987, SLAC-PUB-4206, Stanford, February 1987.
17. S. Kheifets *et al.*, 13th Int. Conf. High Energy Acc., Novosibirsk, U.S.S.R., Aug. 1986, SLAC-PUB-4013.
18. T. Fieguth *et al.*, Studies of Anomalous Dispersion in the SLC Second Order Achromat, Proc. of the 12th Particle Accelerator Conf., Washington, D.C., March 16-19, 1987; SLAC-PUB-4096, Stanford, March 1987.
19. J. J. Murray, K. L. Brown and T. Fieguth, The Completed Design of the Final Focus System, SLAC-PUB-4219, and Proc. of the Particle Accelerator Conf., Washington, D. C., March 16-19, 1987.
20. K. L. Brown, A Conceptual Design of Final Focus Systems for Linear Colliders, SLAC-PUB-4159, and Proc. of the Joint US-CERN School on Particle Accelerators, South Padre, Texas, October 1986.
21. P. Bambade, Beam Dynamics in the Final Focus System, SLAC-PUB-4227, and Proc. of the 12th Particle Accelerator Conf., Washington, D. C., March 16-19, 1987.
22. G. Trilling *et al.*, SLAC-PUB-3561, April 1983.
23. G. Hanson, Nucl. Instr. Meth. A252, 343 (1986).
24. SLD Design Report, SLAC-Report-273, May 1984.
25. Mark II Collaboration and SLC Final Focus Group, Extraction-Line Spectrometer for SLC Energy Measurement, SLAC-SLC-PROP-2, 1986.
26. SLC Polarization Collaboration, Proposal for Polarization at the SLC, Stanford Linear Accelerator Center, Stanford, CA, 1986.